JOURNAL OF OPTOELECTRONICS AND ADVANCED MATERIALS Vol. 10, No. 8, August 2008, p. 2095 - 2099

Modelling the optical gain and noise of Er^{3+}:Ti:$LiNbO_3$ waveguide Mach-Zehnder interferometer

L. A. PUSCAS, E. M. ROTAR, N. N. PUSCAS[a]
Institute for Electrotechnics, Splaiul Unirii, 313, Bucharest, Romania
[a]Physics Department, University "Politehnica" Bucharest, Splaiul Independentei 313, 060042, Bucharest, Romania,

Using a quasi-two-level model in the small gain approximation and the unsaturated regime in this paper we report some original results concerning the evaluation of the spectral optical gain, spectral noise figure and spectral signal-to-noise ratio in the bent Er^{3+}:Ti:$LiNbO_3$ waveguide of the Mach-Zehnder interferometer pumped near 1484 nm using erfc, Gaussian and constant profile of the Er^{3+} ions in $LiNbO_3$ crystal. We demonstrated that rather high gains (~1.5 dB), low noise figures (~3.5 dB) and good signal-to-noise ratios (~56.5) at the end of the bent arm and also, in the straight one of the integrated Mach-Zehnder interferometer are achievable for 70 mW input pump power. The obtained results can be used for the design of the integrated Mach-Zehnder interferometers and other complex optic devices.

(ReceivedNovember 20, 2007; accepted June 30, 2008)

Keywords: Er^{3+}:Ti: $LiNbO_3$ optical waveguides, Integrated Mach-Zehnder interferometer, Gain, Noise figure, Signal-to-noise ratio

1. Introduction

The straight and curved Er^{3+}-doped $LiNbO_3$ optical waveguides are widely used for the fabrication of complex integrated optic components such as: Mach-Zehnder interferometers (MZI), wavelength multiplexers/demultiplexers, high-gain Er^{3+}-doped waveguide amplifiers, doptical switches etc.. Mach-Zehnder integrated interferometers are optical devices which use the interference between two optical signals from the same origin traveling through different effective path lengths. The difference between the effective lengths that the optical signal travels through each arm of the MZI can be induced by making two waveguide with identical response and different physical lengths or by changing dynamically the properties of one of the waveguides (with the same length in this case) resulting in a different phase shift in each path.

In the last years several theoretical and experimental studies have been reported to describe the optical amplification in straight and curved Er^{3+}:Ti:$LiNbO_3$ waveguides [1]-[6]. Various techniques have been proposed to reduce the propagation losses in the bent waveguides and also the overall insertion losses by means of optical amplification in Er^{3+} -doped crystals. However, the amplification behaviour of complex doped structures involving bent waveguides is not well understood, nor described.

In this paper, we propose an original theoretical analysis of the optical amplification on the dopant concentration in the bent Er^{3+}:Ti:$LiNbO_3$ waveguide of the Mach-Zehnder interferometer. The method consists in slicing the curved waveguide in elementary straight sections. In each section, the refractive index profile is calculated, and the optical fields profiles are computed [9]. These data are then injected in a model for straight Er^{3+}:Ti:$LiNbO_3$ amplifiers, in order to calculate the characteristics of the device. Here, we evaluate the spectral optical gain, the spectral noise figure and the spectral signal-to-noise ratio. Simulations are performed under the small gain approximation, for x-cut, z propagating crystals, pumped near 1484 nm, at various pumping regime, dopant concentrations and for different Er concentration profiles in order to obtain the same gain in the two arms of the Mach-Zehnder interferometer and a good visibility of the interference fringes. Although the technique we propose can be applied to any waveguide configuration.

The structure of the paper is as follows. In Section 2, we present the basic equations which describe optical amplification in waveguides, and the expressions of the above mentioned parameters. Section 3 is devoted to the numerical implementation and to the discussion of the simulation results. In Section 4 we present the conclusions of this work.

2. Theory

For the evaluation of the noise characteristics of Er^{3+}-doped $LiNbO_3$ waveguide amplifier we considered a quasi-two-level system model and we neglected excited state absorption due to the considered pumping wavelength [3,5,7]. From the analysis of the interaction of the pump and signal photons with Er^{3+} ions in $LiNbO_3$ it is possible to obtain a system of coupled differential equations for the population densities of the upper laser level and for the pump, signal and amplified spontaneous emission (ASE) field intensity [3,5]. This system was solved numerically in the case of steady state.

Taking into account that the distribution of the photons is not unuiform over the surface of the waveguide the photon mean value $\langle n(z)\rangle$ becomes [3], [5], [7]:

$$\langle n(z)\rangle = G(z)\langle n(0)\rangle + N(z) \tag{1}$$

where:

$$G(z,\nu) = \exp\left\{\int_0^z \left[\gamma_e(z',\nu) - \gamma_a(z',\nu) - \alpha(\nu)\right]dz'\right\} \tag{2}$$

$$N(z,\nu) = G(z,\nu)\int_0^z \frac{\gamma_e(z',\nu)}{G(z',\nu)}dz' \tag{3}$$

represent the spectral gain and the ASE photon number, respectively. In Eqs. (1)-(3)

$$\gamma_e = \gamma_e(z,\nu) = \sigma_e(\nu)\int_A N_2(x,y,z) i_m(x,y)dxdy \tag{4}$$

$$\gamma_a = \gamma_a(z,\nu) = \sigma_a(\nu)\int_A N_1(x,y,z) i_m(x,y)dxdy\,. \tag{5}$$

In the case of large gain (i. e. $G(z) >> 1$) the noise figure is given by [4, 5]:

$$F(z,\nu) = \frac{1+2N(z,\nu)}{G(z,\nu)} \tag{6}$$

where the term $\frac{2N}{G}$ corresponds to a beat noise regime at the peak gain and the term $\frac{1}{G}$ to a shot noise at the spectrum tails.

Taking into account the photon statistics master equation of the linear amplifier and assuming signal injection at z=0, based on the model presented in papers [3], [5], [7] we calculated the gain $G(L,\nu)$ and the ASE noise $N(L,\nu)$ at the output of the amplifier.

The noise figure and the signal-to-noise ratio at the output of the amplifier are given by:

$$F(L,\nu) = \frac{1+2G(L,\nu)\int_0^L \frac{\gamma_e(z',\nu)}{G(z',\nu)}dz'}{G(L,\nu)} \tag{7}$$

$$SNR(L,\nu) = \frac{n(0)G(L,\nu)}{1+2G(L,\nu)\int_0^L \frac{\gamma_e(z',\nu)}{G(z',\nu)}dz'} \tag{8}$$

When deriving the relations of the gain, ASE photon number, noise figure and signal-to-noise ratio at the output of the device (Eqs. (2), (3), (7) and (8)), an input signal with Poisson statistics $\left(\sigma^2(0) = \langle n(0)\rangle\right)$ has been considered. In order to evaluate the optical mode profiles in the case of bent waveguides we sliced the bent waveguide in elementary portions, each of them being considered straight, and tilted at an angle θ with respect to the "z" axis (Fig. 1 a)). At each propagation step (corresponding to a particular angle θ), and for both TM and TE polarisations, we calculated the refractive index profiles using the Fick's diffusion law [6], [9]. For TM polarised waves (oriented along the "x" axis), only the ordinary refractive index is concerned. Therefore, the refractive index profile does not depend on the angle θ. It is given by:

$$n(x,y') = n_0 + \Delta n_0 \exp\left(-\frac{x^2}{a^2}\right)\left\{\mathrm{erf}\left(\frac{w+2y'}{a}\right) + \mathrm{erf}\left(\frac{w-2y'}{a}\right)\right\} \tag{9}$$

where n_0 is the ordinary refractive index, Δn_0 is the surface refractive index variation due to the Ti diffusion, w is the waveguide width, and y' is the transverse coordinate of the tilted waveguide as seen from Fig. 1 a), "a" is a parameter which depends on the diffusion conditions. It is given by $a = 2\sqrt{Dt}$, where D and t are the diffusion constant and time respectively. It is usually considered that the diffusion constant is the same in the "x" and "y" directions.

On the contrary, for TE polarised waves (oriented along the "y' " axis), the refractive index profile involves both the ordinary and the extraordinary indices, and it does depend on the angle θ. It is given by:

$$n(x,y',\theta) = n_s(\theta) + \Delta n(\theta)\left[\exp\left(-\frac{x^2}{a^2}\right)\right]\times \times\left\{\mathrm{erf}\left(\frac{w+2y'}{a}\right) + \mathrm{erf}\left(\frac{w-2y'}{a}\right)\right\} \tag{10}$$

where

$$\Delta n(\theta) = \frac{n_0^3 \Delta n_e \sin^2\theta + n_e^3 \Delta n_0 \cos^2\theta}{\left(n_e^2\cos^2\theta + n_0^2\sin^2\theta\right)^{3/2}} \tag{11}$$

and

$$n_s(\theta) = \frac{n_0 n_e}{\left(n_e^2\cos^2\theta + n_0^2\sin^2\theta\right)^{1/2}}\,. \tag{12}$$

In order to account for the waveguide curvature, we refer to Fig. 1 b). In a curved waveguide, the inner part of the wavefront propagates over a shorter distance than its outer part. For the light, it looks as if the refractive index were lower in the inner part than in the outer part of the waveguide. This can be accounted for in the expression of the refractive index profile by using the following conform transformation:

$$n_c(x,y') = n(x,y')\left(1+\frac{y'-R}{R}\right) \qquad (13)$$

where R is the radius of curvature of the waveguide.

The system of coupled differential equations for the population densities of the upper laser level and for the pump, signal and ASE powers were integrated with an iterative procedure, using a Runge-Kutta formula (4 th order, 4 stages), the iterations being stopped when the change in the power of the about mentioned fields is smaller than a prescribed value.

In our model the intensity profiles $i_m(x,y)$, for both TE and TM polarisations were calculated numerically with the method described above, while the dopant distribution was approximated by a constant, but also by erfc or Gaussian functions in depth, and a Gaussian function in width which correspond to different diffusion conditions or crystal fabrications. An erfc profile is obtained when the diffusion of the Er ions is not completed, while a Gaussian profile corresponds to case where all the Er ions have diffused into the crystal. The last case (constant in depth) corresponds to the case where the crystal is doped with Er during the growth process.

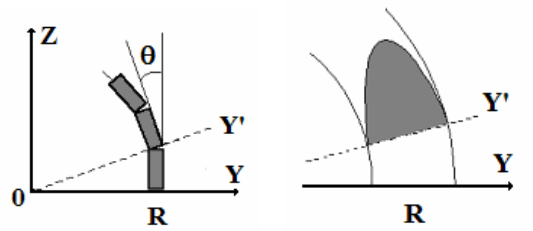

a) b)

Fig. 1a), b). Parameters used for the calculation of the mode profiles. a) Decomposition of the guide in elementary slices; R radius of curvature, Z longitudinal coordinate, Y transverse coordinate, Y' transverse coordinate of an elementary slice, and θ orientation of the elementary slice, b) In a bent waveguide, the inner part of the wavefront propagates over a shorter distance than its outer part.

3. Discussion of the simulation results

We have computed the spectral dependence of the gain, noise figure and signal-to-noise ratio for the bent Er^{3+}-doped $LiNbO_3$ waveguide (1) of the Mach-Zehnder interferometer (Fig. 2) with signal and pump wavelengths of 1531 nm and 1484 nm, respectively for several concentrations of the dopant.

For the numerical simulation, we used parameters obtained from the literature [5], [6], [8]. We found that the Er^{3+} surface concentrations during growth is about $12\times10^{26}\ \mathrm{m}^{-3}$ in the bent arm and about $3.9\times10^{25}\ \mathrm{m}^{-3}$ in the straight arm, respectively (in order to obtain the same gain in the two arms and a good visibility of the interference fringes). Various diffusion depths or profiles have been considered. We assumed the following values for the scattering losses and spontaneous emission lifetime: α=0.4 $\mathrm{dB\cdot cm^{-1}}$ and α=0.2 $\mathrm{dB\cdot cm^{-1}}$ for the bent arm and straight one, respectively, for both TE and TM polarizations and τ=2.6 ms. The radius of curvature of the bent waveguide is R=4.8 cm, $\beta = 9^o$, the length of the straight waveguide is l=1 cm. The pump or signal were assumed to be TE polarized if not explicitly stated. In the following results, curves labelled 1, 2 and 3, refer respectively to Er^{3+} ions profiles in erfc function, Gaussian function and constant in depth. In computing the profile of the optical modes using Eqs. (9)-(13) we used the following parameters characteristic of Ti waveguides: 6 μm for waveguide width, 0.1 μm for Ti thickness, 10 hours for diffusion time, 6 μm and 6 μm for modal dimensions in width and depth [6].

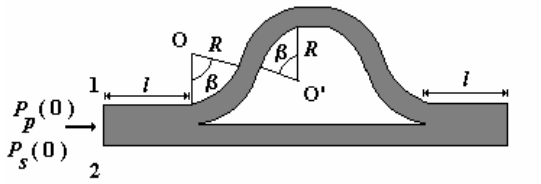

Fig. 2. The Er^{3+}:Ti:$LiNbO_3$ waveguide Mach-Zehnder interferometer.

Figs. 3 a), b), c) present the evolution of the gain spectra, $G(z) = \ln\left[P_{signal}(z)/P_{signal}(0)\right]$, noise figure, and signal-to-noise ratio respectively for input pump powers of 70 mW considering an Er^{3+} diffusion depth of 20 μm and a concentration of about $12\times10^{25}\ \mathrm{m}^{-3}$.

As can be seen from Figs 3 a), b) and c) in the case of the above mentioned conditions it is possible to obtain rather high gains (i. e. 1.48 dB and 1.14 dB), low noise figures (i. e. 3.54 and 3.05 dB and good signal-to-noise ratios (i. e. 56.52 and 55.72) for Gaussian and erfc, respectively profiles in depth and Gaussian profiles in width in TE polarization at the end of the Mach-Zehnder interferometer.

The dependences of the gain, noise figure and signal-to-noise ration on the Er^{3+} ions concentration in the case of Gaussian profile in width of the dopant and 50 mW input

pump power for the bent arm of the Mach-Zehnder interferometer are presented in Figs. 4 a), b), c).

In the case of the above mentioned conditions the highest values of the gain are: 1.55 dB, 1.56 dB and 1.49 dB for the folowing values of the concentrations: 30×10^{25} m^{-3}, 25×10^{25} m^{-3}, 20×10^{25} m^{-3} of the dopant in the depth of the waveguide and the folowing profiles: erfc, Gaussian and constant, respectively.

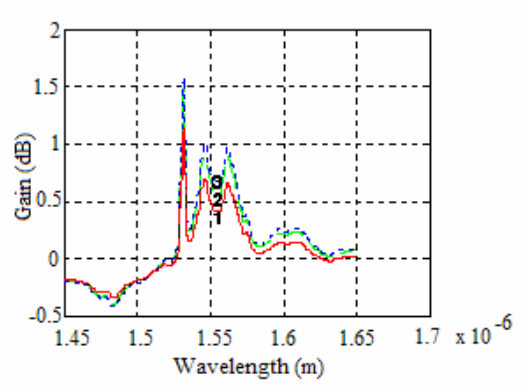

a)

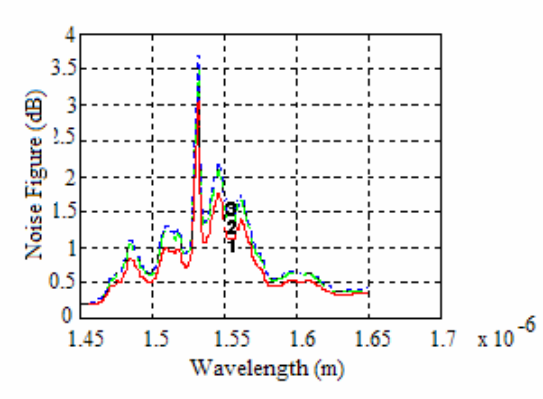

b)

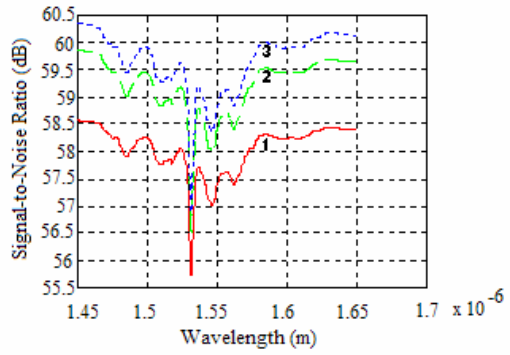

c)

Fig. 3 a), b). a) Spectral gain, b) spectral noise figure and spectral signal-to-noise ratio.

For concentrations much higher than 10^{26} m^{-3} the undesirable effect of clusters formation begins to appear.

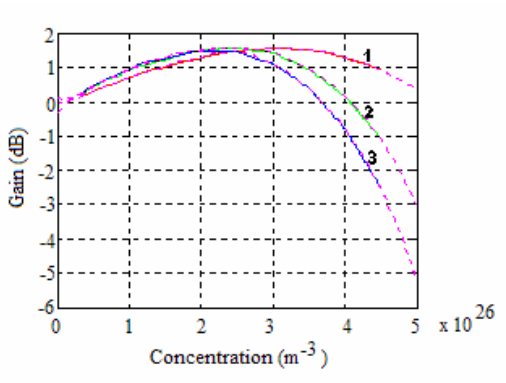

a)

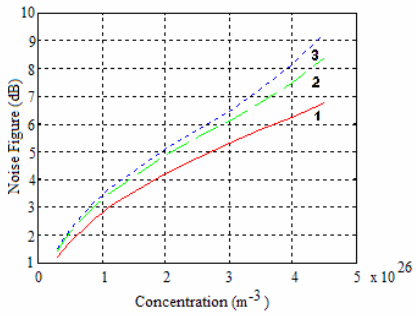

b)

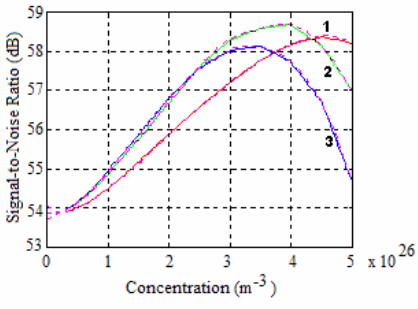

c)

Fig. 4 a), b). c). a) The dependences of the: a) gain, b) noise figure and c) signal-to-noise ratio vs the dopant concentration.

The dependences of the gain, noise figure and signal-to-noise ratio on the pump power in the case of Gaussian profile in width and a concentration of the dopant of about 25×10^{25} m^{-3} for the bent arm of the Mach-Zehnder interferometer are presented in Figs. 5 a), b), c).

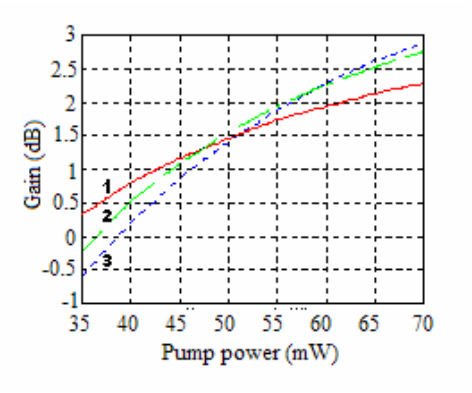

a)

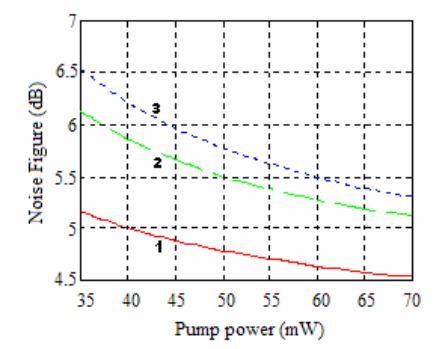

b)

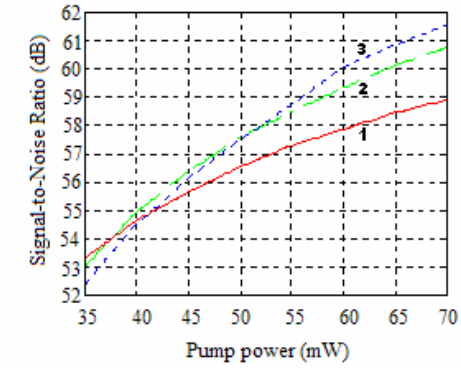

c)

Fig. 5 a), b), c). a) The gain, b) noise figure and signal-to-noise ratio vs pump power.

As can be seen from Figs. 5 a), b) and c) the increase of the pump power enhances the gain and the signal-to-noise ratio and produce a decrease of the noise figure for all the profiles of the dopant in the depth of the waveguide.

4. Conclusions

In this paper we have presented a theoretical analysis and an accurate evaluation of the spectral optical gain, spectral noise figure and spectral signal-to-noise ratio for the bent Er^{3+}-doped $LiNbO_3$ waveguide of the Mach-Zehnder interferometer pumped at 1484 nm.

The theoretical analysis was made using the small gain approximation in the unsaturated pump regime. From the behaviour of the above mentioned parameters, under various pumping regimes and dopant concentrations, we have demonstrated that rather high gains, low noise figures and good signal-to-noise ratios are achievable in high pump regimes.

This emphasizes the interest of our method for the design of complex doped structures. It must be noted that the method can be applied to any waveguide architectures and rare earth diffusion conditions. This technique can be used for the design of a lossless and large path imbalance Mach-Zehnder interferometer with enhanced visibility. However, more complex rare earth doped integrated structures can be designed using the above mentioned method.

References

[1] I. Mansour, F. Caccavale. Applied Optics **35**, 1492 (1996).
[2] J. De Merlier, D. Van Thourhout, G. Morthier, R. Baets, IEEE Journ. of Quant. El. **39**(9) 1099 (2003).
[3] I. Baumann, R. Brinkmann, M. Dinand W. Sohler, S. Westenhofer, IEEE J. Quant. Electron., **QE 32**, 1695-1706 (1996).
[4] P. Ganguly, J. C. Biswas, S. K. Lahiri. Fiber and Integrated Optics **24**, 511 (2005).
[5] N. N. Puscas, R. Girardi, D. Scarano, I. Montrosset. Journ. Mod. Optics **45**, 847 (1998).
[6] N. N. Puscas, B. Wacogne, A. Ducariu, B. Grappe, Opt. and Quant. Electronics **32**, 1 (2000).
[7] E. Desurvire, Erbium-Doped Fiber Amplifiers, J. Wiley & Sons, Inc. New York (1994).
[8] N. N. Puscas, A. Ducariu, G. C. Constantin, D. Dinu, J. Optoelectron. Adv. Mater. **7**(2), 1057 (2005).
[9] D. Marcuse, Light Transmission Optics, Van Nostrand, New York (1972).

*Corresponding author: pnt@ physics.pub.ro